



## EXPERIMENTAL TEST FOR STRUCTURAL PERFORMANCE EVALUATION OF R/C MEMBERS ASSUMING RENOVATION

R. Takahashi<sup>(1)</sup>, T. Mukai<sup>(2)</sup>, Y. Maida<sup>(3)</sup>, H. Kinugasa<sup>(4)</sup>

<sup>(1)</sup> Graduate Student, Tokyo University of Science, 7119551@ed.tus.ac.jp

<sup>(2)</sup> Senior Research Engineer, Building Research Institute, t\_mukai@kenken.go.jp

<sup>(3)</sup> Researcher, National Institute for Land and Infrastructure Management, maida-y92gy@mlit.go.jp

<sup>(4)</sup> Professor, Tokyo University of Science, kinu@rs.noda.tus.ac.jp

### Abstract

It has been confirmed that reinforced concrete box-shaped wall structures, many of which were constructed in the 1970s, have high seismic performance, since those houses suffered almost no damage in subsequent major earthquakes. However, those houses have the problem that the area of each dwelling unit is small and does not meet the needs of current users. Remedial measures are to make a new opening in a boundary structural wall with an adjacent room, to improve the functionality of house. However, it is expected that seismic performance deteriorates due to a new opening on a boundary structural wall, countermeasure should be needed.

The purpose of this study is to propose appropriate methods for reinforcing a structural wall with a new opening and a wall girder on top of the opening, and an evaluation method for the structural performance of those structural members when a new opening is made in a reinforced concrete box-shaped wall structure, through experimental tests.

An opening was made in an existing structural wall, and then the structural wall was reinforced by additionally post-placing concrete, using some post-installed adhesive anchors as reinforcement at the wall edge. Then, a structural experimental test on the structural wall was carried out. Regarding this test, the diameter and the number of newly installed reinforcing bars and the strength of the additionally-placed concrete were used as variable parameters. On the other hand, an experimental test on a wall girder was carried out. The wall girder was reinforced by newly installed flexural reinforcement and shear reinforcement on both sides of the girder, and additionally placed concrete. In this test, a method for arranging shear reinforcing bars was used as a parameter.

It was confirmed that the backbone curve of horizontal load–deformation relationship between the structural wall and the wall girder with the reinforcing bars could be evaluated accurately in general by the past calculation formula through these experimental tests. Moreover, it was confirmed that the ductility performance of the structural wall was improved, especially in the case which the high strength concrete additionally placed at the wall edge. In addition to that, it was confirmed that the same strength could be obtained by increasing the diameter of the reinforcing bars, even if the number of reinforcing bars where were newly installed was decreased. On the other hand, it was confirmed that the method of arranging shear reinforcement bars for the wall girder affected the ductility performance.

*Keywords: Renovation, Reinforced Concrete; Box-shaped wall structure; Structural wall; Wall girder; Backbone curve*



## 1. Introduction

Many reinforced concrete (RC) box-shaped wall apartment buildings constructed from the mid-1960s to late 1970s no longer meet today's housing needs such as larger areas for living. The remedial measures include reducing the beam depth and making a new opening in an existing boundary structural wall. Because these methods deteriorate seismic performance, the components around openings need to be reinforced. However, there is not sufficient knowledge of the methods for reinforcing those components and for evaluating their structural characteristics after reinforcement. Hibino et al. [1] proposed a method for reinforcement against the reduction in beam depth and reviewed its effectiveness by experiment. They reported that it is possible to keep flexural strength, shearing strength, and rigidity by installing RC beams on both sides of the beam that was cut off or reinforcing both or either side of the beam that was cut off with steel beams. Maruyama et al. [2] proposed the method for reinforcing a structural wall with the shorter spans around an opening and reviewed its effectiveness by experiment. They reported that by using post-installed adhesive anchors for flexural reinforcement, it is possible to obtain seismic performance similar to prefabricated rebars.

The purpose of this research is to elucidate the effects of reinforcement and the methods for evaluating structural performance by conducting experiments on reinforced wall girders and a long-span structural wall used for installing new openings in an existing boundary structural wall of an RC box-shaped wall structure and then analyzing the results.

## 2. Experiment on Wall Girders Reinforced for Installing an Opening

### 2.1 Outline of the Test Pieces

Table 1 lists the outline of the test pieces, Table 2 shows the results of testing the concrete materials used, and Table 3 the results of testing the steel frame materials used. In addition, Fig. 1 contains a bar arrangement drawing of the test pieces. Two test pieces were prepared. The test targets were the wall girders at the top of a new opening in an existing boundary structural wall. These test pieces were existing wall girders with both sides newly reinforced with shear reinforcement (D10@100) and flexural reinforcement (4-D16); then, concrete was placed. Lastly, the additional part and the existing part were connected with bolts for reinforcement. The two test pieces had different arrangements of the newly installed shearing reinforcement. Test piece B-2' had a separate vertical rebar on both sides as an alternative to shearing reinforcement. In the case of test piece B-3', a U-shaped shearing reinforcement rebar surrounding the existing wall girders was installed after chipping the concrete at the lower part of the wall girder more than that of test piece B-2'. The slab widths of the test pieces were approximately 1 m, which is generally effective for improving flexural strength, while considering fitting into the testing device.

### 2.2 Force Application Measurement Plan

Fig. 2 shows the setup of the force-application device. The force-application method was positive and negative alternative repeated loading with a cantilever with a contraflexure point height of 600 mm above the bottom stub. The direction of the positive load was the direction of compressing the slab, and the force-application cycle was interlayer deformation angle control. The deformation angles of the measurement cycles were  $R = 0.06, 0.13, 0.25, 0.50, 0.75, 1.00, 1.49, 2.00,$  and  $3.03\%$ , with each cycle repeated up to twice. The axial force was 0. Fig. 3 indicates the position of the strain gauge used in Section 2.4 "Discussion." For measurement, strains are measured with a strain gauge, the deformation of rebars are measured with a deformation gauge, and the widths and progress of cracks are visually observed and by photographs. Also, the amount of damage including flaking and lifting are measured using overhead projector (OHP) sheets. In addition, with a measurement frame installed outside each test piece, the relative deformation angles of the force-application position and critical section position are measured and used for controlling force applications.

### 2.3 Results of the Experiment

Fig. 4 illustrates the relationship between load and deformation angle and plots the position at which each rebar yields. In test piece B-2', it was the existing flexural reinforcement in the girders that first reached tensile



yield strain at  $R = 0.293\%$  on the positive load side. On the side of the negative load, the slab rebars first reached tensile yield strain at  $R = 0.247\%$ . Then, at  $R = 2.017\%$ , vertical cracks were found at the boundary between the reinforced part and existing part, indicating a reduction in yield strength. The maximum yield strength was 233.3 kN at  $R = 0.483\%$  on the positive load side and was -353.9 kN at  $R = -2.17\%$  on the negative load side.

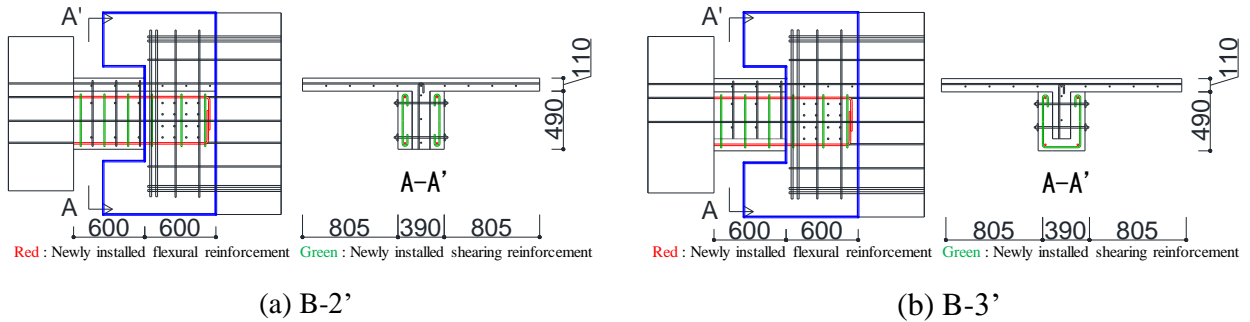


Fig. 1 A bar arrangement drawing of the test pieces

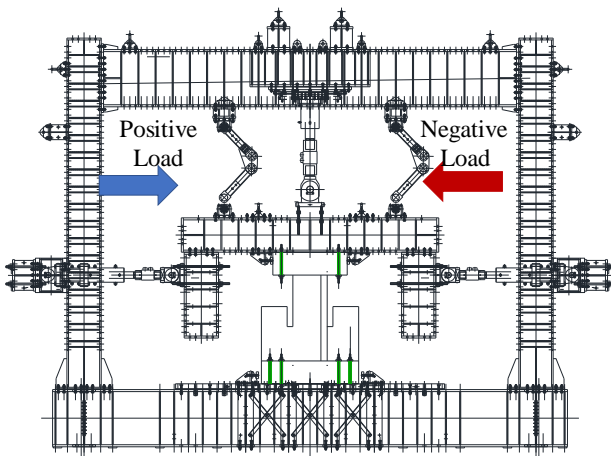


Fig. 2 The setup of the force-application device

Table 1 The outline of the test pieces

Test piece	B-2'	B-3'
Beam depth(mm)	600	
Beam width(mm)	390	
Length of beam(mm)	600	
Existing main reinforcement	D10(SD295A)	
Newly installed flexural reinforcement	2-D16(SD345)	
Existing shearing reinforcement	D10(SD295)@200	
Newly installed shearing reinforcement	D10(SD295)@200 vertical rebar U-shaped rebar	
Slab thickness(mm)	110	
Slab width(mm)	805	
Slab reinforcement	D10(SD295)	
Bolt(Hole diameter18mm)	M16	
Existing concrete strength(N/mm <sup>2</sup> )	18	
Newly installed concrete strength(N/mm <sup>2</sup> )	27	

Table 2 The results of testing the concrete materials

Part	Specified design strength (N/mm <sup>2</sup> )	Young's modulus (N/mm <sup>2</sup> )	Compressive strength (N/mm <sup>2</sup> )	Tensile strength (N/mm <sup>2</sup> )
Existing part	18	23324	20.9	1.91
Reinforced part	27	29343	37.1	2.86

Table 3 The results of testing the steel frame materials

Reinforcement	Young's modulus $\times 10^3$ (N/mm <sup>2</sup> )	Yield strength (N/mm <sup>2</sup> )	Yield strain ( $\mu$ )	Tensile strength (N/mm <sup>2</sup> )
D10	187	356	1995	489
D16	185	372	2062	543

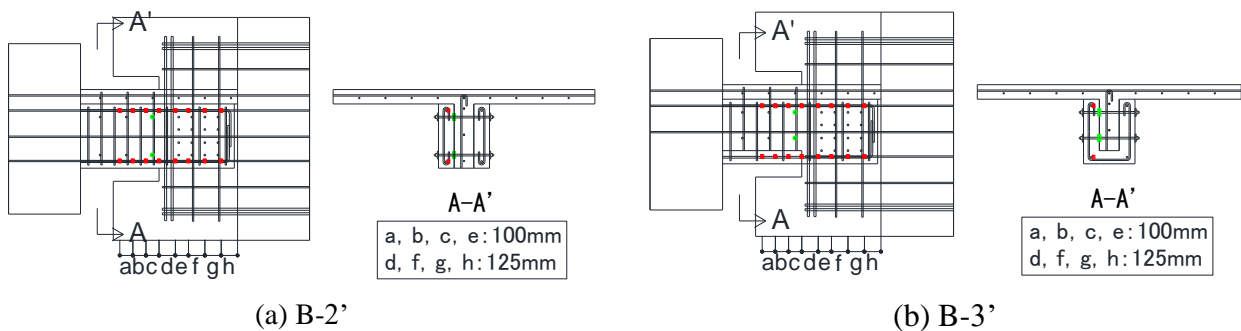


Fig. 3 The position of the strain gauge



For B-3', the new flexural reinforcement in the girders first reached tensile yield strain at  $R = 0.117\%$  on the positive load side, and the slab rebars first reached tensile yield strain at  $R = -0.157\%$  on the side negative loading side. At  $R = -1.527\%$ , girder ends significantly flaked off, resulting in a decrease in yield strength. The maximum yield strength was 227.8 kN at  $R = 2.783\%$  on the positive load side and -256.7 kN at  $R = -0.58\%$  on the negative loading side.

## 2.4 Discussion

### 2.4.1 Failure Mode of Each Test Piece

#### (1) B-2'

On the side of the positive load, after the yielding of the existing and the new flexural reinforcements in the girders, the new shearing reinforcement installed in the girders yielded, but the yield strength did not immediately decrease. At a deformation angle,  $R$  of around 3%, shear cracks widened, followed with a sudden drop in yielding strength. The series of events suggests that a shear failure eventually occurred, but after the yielding of the new flexural reinforcement. Thus, the ultimate failure mode was a shear failure after flexural yield. On the side of the negative load, after the yielding of slab rebars and the existing and the new flexural reinforcements in the girders, the existing shearing reinforcement in the girders yielded, but the yield strength did not suddenly drop. Afterward, there was no reduction in yield strength involving the widening of shear cracks and yielding of shearing reinforcement. Therefore, the ultimate failure mode was a flexural failure.

#### (2) B-3'

On the positive load side, similar to B-2', after the yielding of the existing and new flexural reinforcements in the girders, the new shearing reinforcement installed in the girders yielded, but the yield strength did not immediately decrease. At a deformation angle,  $R$  of around 3%, shear cracks widened, followed with a sudden decrease in yielding strength. The series of events suggests that a shear failure eventually occurred, but it was after the yielding of the new flexural reinforcement. Consequently, the ultimate failure mode was a shear failure after flexural yield. On the side of the negative load, after the yielding of slab rebars and the existing and new flexural reinforcements in the girders, the existing and new shearing reinforcement in the girders yielded, but the yield strength did not suddenly drop. Afterward, at a deformation angle,  $R = -1.527\%$ , the concrete at the girder ends flaked off, resulting in a sudden decrease in yield strength. Therefore, the ultimate failure mode was a flexural compressive failure following flexural yielding.

### 2.4.2 Positions of the critical sections of B-2' and B-3'

Fig. 5 shows the curvature distribution at a distribution angle of  $R = -0.06\%$ . The measurements by a strain gauge were used to obtain the curvatures by calculation. There were significant differences in failure modes and yield strengths between B-2' and B-3' on the side of the negative load. The reason for these differences is possibly the outstanding curvature of B-3' at 125 mm inside the stub, as indicated in Fig. 10, resulting in the critical section located deep inside the stub. The reason for the aforementioned results is that test pieces B-2'

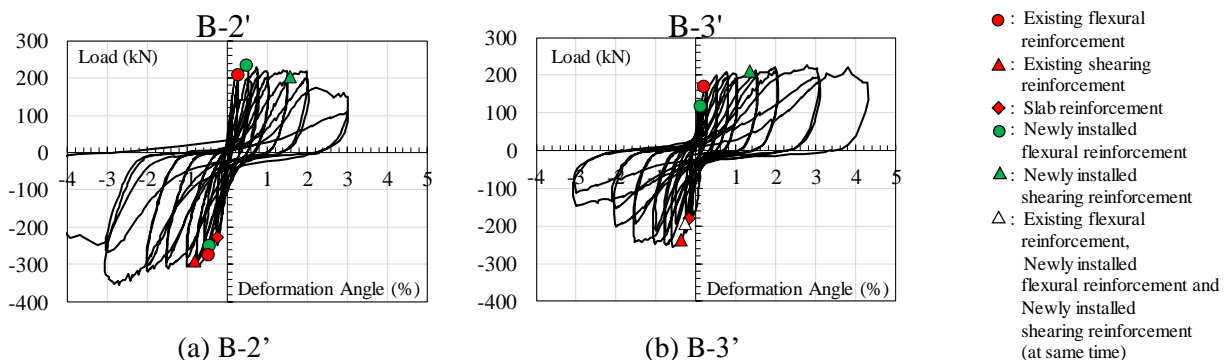


Fig. 4 The relationship between load and deformation angle



and B-3' were prepared by repairing wall girder-structural wall joint test pieces, but it seems that B-3' was not properly repaired. In the case of B-2', the part of the structural wall was broken off and concrete with a strength higher than that of the girder was placed to form a new stub. In the case of B-3', additional concrete was placed without removing the structural wall, leaving the structural wall inside the new slab. Such faulty repair resulted in the critical section located inside the stub. In Fig. 10 showing B-2' before repair, the critical section was positioned inside the junction between the wall girder and structural wall. However, after repair, it was not located inside, suggesting that B-2' was properly repaired.

#### 2.4.3 Evaluation of the backbone curves concerning load deformation

For the evaluation of the yield strength of reinforced wall girders, the accuracy of evaluation expressions indicated in [3–5] was determined. Fig. 6 compares the calculated backbone curves and experimental values, and Table 4 lists the accuracy of the calculated values. The flexural ultimate strength of the backbone curves was obtained using the precise calculation method, or Eq. (1) presented in [4]. The shearing ultimate strength was provided using Eq. (2) presented in [5]. The flexural crack strength, shear crack strength, and yield point rigidity reduction rate were obtained by calculation using Eqs. (4–6), respectively, as indicated in [3]. As mentioned in Section 2.4.2, the calculation assumed that the critical point was 125 mm inside the stub for the negative load on B-3'.

$$M_u = A_{st}\sigma_{st}d - A_{sc}\sigma_{sc}d_c - \frac{\sigma_{av}b\beta_1x_n}{2} \quad (1)$$

Here,  $A_{st}$ : Cross-sectional area of each rebar on the pulling side of the neutral axis including the cross-sectional area of the slab reinforcement within the effective range (a width of 1 m);  $\sigma_{st}$ : Strength of the material of the rebars on the pulling side of the neutral axis;  $d$ : Distance from the compression edge to each rebar on the pulling side;  $A_{sc}$ : Cross-sectional area of each rebar on the compression side of the neutral axis;  $\sigma_{sc}$ : Strength of the material of the rebars on the compression side of the neutral axis;  $d_c$ : Distance from the compression edge to each rebar on the compression side;  $\beta_1$ : A coefficient of 0.85;  $x_n$ : Distance from the compression edge to the neutral axis;  $\sigma_{av}$ : The average intensity of stress of the concrete.

$$Q_u = \frac{0.068p_{te}^{0.23}(F_c+18)}{M/Qd+0.12} + 0.85\sqrt{p_{we}\sigma_{wy}}\}b_ej \quad (2)$$

Here,  $p_{te}$ : The ratio of the tension reinforcement, which is the part from the pulling edge to the center of gravity of the reinforcement, including the slab reinforcement within the effective range (a width of 1 m) if the slab is connected to the pulling side;  $b_e$ : Equivalent width, not exceeding 1.2b;  $d$ : Effective height;  $F_c$ : The strength of the concrete;  $M/Qd$ : Shear span ratio with  $1 \leq M/Qd \leq 3$ ;  $p_{we}$ : Equivalent vertical reinforcement ratio, not exceeding 1%;  $\sigma_{wy}$ : Standard yield point of the shear reinforcement;  $j$ : Distance between the center of tension and the center of the compression.

$$K = \frac{1}{\frac{L^3}{3E_cI_e} + \frac{\kappa L}{GA}} \quad (3)$$

Here,  $L$ : Length of the component;  $E_c$ : Young's modulus of the concrete;  $I_e$ : Equivalent cross-sectional secondary moment;  $G$ : Shear elastic modulus;  $A$ : Cross-sectional area of the component;  $\kappa$ : Shear form factor, which is 1.2.

$$M = (0.56\sqrt{\sigma_B})Z_e \quad (4)$$

Here,  $Z_e$ : Equivalent cross-sectional coefficient;  $\sigma_B$ : Compressive strength of the concrete, which is the design standard strength.

$$Q = \tau_{scr} \cdot b \cdot D/\kappa \quad (5)$$

Here,  $\tau_{scr}$ : Shear crack strength of the concrete;  $b$ : Girder width;  $D$ : Girder height;  $\kappa$ : Shear form factor, which is 1.2.

$$\alpha_y = (0.043 + 1.64n \cdot p_t + 0.043 \cdot \frac{M}{Qd}) \cdot (\frac{d}{D})^2 \quad (6)$$

Here,  $n$ : Young's modulus ratio between the concrete and reinforcement;  $p_t$ : The ratio of the tension



reinforcement, which is the part from the pulling edge to the center of gravity of the reinforcement, including the slab reinforcement within the effective range if the slab is connected to the pulling side;  $M/Qd$ : Shear span ratio;  $D$ : Girder height;  $d$ : Effective girder height

When comparing the maximum yield strength between the experimental values and the calculated values, the maximum yield strength in the experimental values can be evaluated on the safe side except under the negative load on B-1.

#### 2.4.4 Toughness of B-2' and B-3' under the Positive Load

Fig. 7 shows the relationship between the strain and the deformation angle of the bolt at 50 mm from the critical section. Under the positive load, B-3' exhibited higher toughness than B-2'. As described in 4.4, on B-2', cracks occurred between the reinforced part and existing part at deformation angle  $R = 2.017\%$ , followed by a reduction in yield strength. Therefore, the shearing between the two parts resulted in lower toughness of B-2'. In addition, for B-2', the bolt that crimps the two parts together had higher strain, indicating a greater difference in behavior between the reinforced part and the new part than that of B-3'.

### 3. Post-Installed Anchor Removal Test

#### 3.1 Outline of the Test Pieces

For the three pieces of anchor reinforcement (a, b, and c) installed as test piece TYPE-A2 stubs in the structural wall experiment in Section 4, a removal test was conducted. A  $\phi 16$ -hole was drilled perpendicularly to the surface of each stub using a hand-held core drill. For anchor reinforcement, D13 (type SD785) high-strength reinforcing bars were used. The anchor reinforcement was buried  $5d_a$  ( $d_a$ : anchor nominal diameter) deep. For anchor reinforcement spacing, a-b was 160 mm and b-c was 100 mm. The end distance of each test piece was 100 mm.

#### 3.2 Force Application Measurement Plan

Fig 8 shows the tensile testing machine. The load was applied by converting hydraulic pressure generated by

Table 4 The accuracy of the calculated values

Test piece	Loading direction	Failure mode	Maximum load (kN)	Calculated value		Accuracy (Experimental value /calculated value)
				Flexural ultimate strength (kN)	Shear ultimate strength (kN)	
B-2'	Positive load	Shear failure following flexural yielding	233.30	207.45	416.69	1.12
	Negative load	Flexural failure	-353.90	-311.40	-571.02	1.14
B-3'	Positive load	Shear failure following flexural yielding	227.80	185.34	404.02	1.23
	Negative load	Flexural compressive failure following flexural yielding	-256.70	-255.34	-506.52	1.01

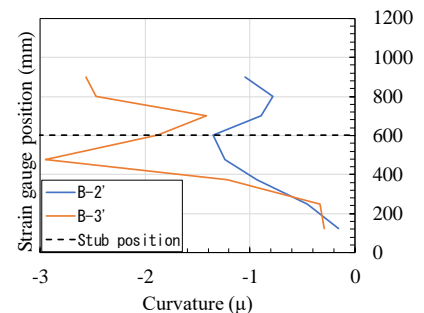
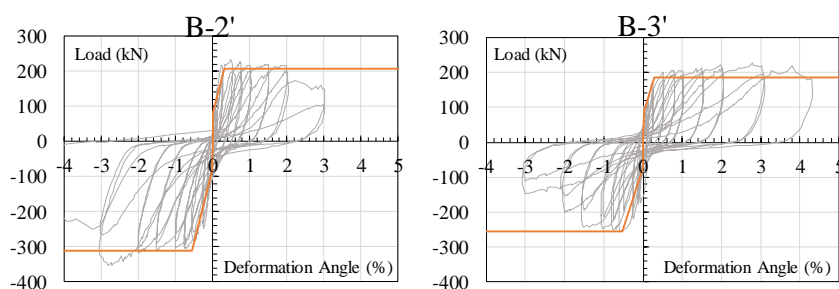


Fig. 5 The curvature distribution



(a) B-2'

(b) B-3'

Fig. 6 The calculated backbone curves

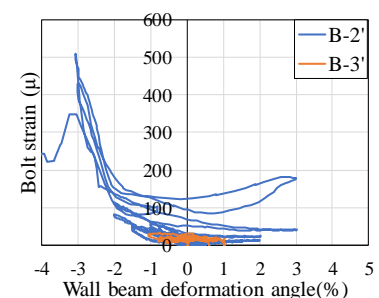


Fig. 7 The bolt strain



a pump into a tensile force and measured with an oil pressure gauge. The deformation was measured on the upper surface of a deformation measurement jig using a displacement gauge.

### 3.3 Results of the Experiment

Table 5 lists the result of the removal test. The bond strength was obtained by dividing the maximum yield strength by the side area of the rebar calculated from the nominal diameter and burying depth of the anchor.

The average bond strength was 25.5 N/mm<sup>2</sup>, and the deformation at the load end at the maximum yield strength was 1.7 to 3.2 mm.

## 4. Experiment on a Structural Wall Reinforced for Installing an Opening

### 4.1 Outline of the Test Pieces

Table 6 shows the outline of the test pieces, Table 7 shows the results of testing the concrete materials used, and Table 8 shows the results of testing the steel frame materials used. Fig. 9 contains the bar arrangement drawing of the test pieces, and three test pieces were prepared. The test targets were the structural walls by the new opening in a boundary structural wall. These test pieces were created by chipping the part of the structural wall that was the edge of the new opening and reinforcing with post-installed as flexural reinforcement. Concrete was then placed on the chipped edge of the opening. To suppress the shear between the part additionally placed and the existing part, horizontal post-installed anchors were used horizontally as joint reinforcement. The effective burying depth of the horizontal post-installed anchors was 15da, and that of the vertical post-installed anchors was 20da. Concerning the parameters of the test pieces described in the reinforcement details, for TYPE-A2 and TYPE-B, the design standard strength of the concrete placed was 27 N/mm<sup>2</sup>, while that for TYPE-A1 was 60 N/mm<sup>2</sup>. The flexural reinforcement of the reinforced part of TYPE-A2 and TYPE-A1 was 3-D16, and that of TYPE-B was 2-D19.

### 4.2 Force Application Measurement Plan

Fig. 10 shows the setup of the force-application device. The force-application method is positive and negative alternative repeated loading with a cantilever with a contraflexure point with a height of 2500 mm above the bottom stub. The direction of the positive load is the direction of compressing the orthogonal wall, but for only TYPE-B, the loading direction was opposite. The force-application cycle is the interlayer deformation angle control. The deformation angles of the measurement cycles were R = 0.06, 0.13, 0.25, 0.50, 0.75, 1.00, 1.49, 2.00, and 3.03%, with each cycle repeated up to two times. A constant axial force with an axial force ratio of 0.075 was applied.

Fig. 11 indicates the position of the strain gauge in the reinforced part. For measurement, displacements were measured with a displacement gauge, the strains of the rebars were measured with a strain gauge, and the widths and progress of cracks were measured visually and by photographs. Also, the damage including flaking and lifting were measured using OHP sheets. In addition, with a measurement frame installed outside each test piece, the relative deformation angles of the force-application position and critical section position were measured and used for the controlling force application.

### 4.3 Results of the Experiment

Fig. 12 illustrates the relationship between load and deformation angle and plots the position at which each rebar yields. In TYPE-A1, the vertical reinforcement in the structural wall first reached a tensile yield point at

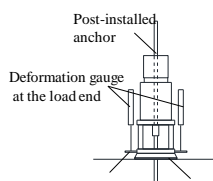


Fig 8 The tensile testing machine

Table 5 The result of the removal test

Test piece	Maximum strength(kN)	Deformation at the maximum strength	Bond strength
a	75	1.7	28.3
b	69.4	1.4	26.1
c	58.6	3.2	22.1



R = 0.08%, followed by the post-installed anchor reinforcement at R=0.11% on the positive load side. On the side of the negative load, the hoop reinforcement first reached a tensile yield point at R = -0.42%. Then, during the first cycle at R = -2.00%, crushing occurred with large shear cracks at the center of the structural wall, resulting in a sudden reduction in yield strength. The maximum yield strength was 749.7 kN at R = 0.73% on the positive load side and -1175 kN at R = -0.73% on the negative load side. On both positive and negative load sides, a failure mode was reached at the calculated values of the flexural strength. However, on the side of the negative load, an abrupt reduction in yield strength because of the widening of shear cracks was found. Therefore, the failure mode on the positive load side was a flexural failure, while that on the negative load side was a shear failure following flexural yielding.

For TYPE-A2, the vertical reinforcement in the structural wall first reached a tensile yield point at R =

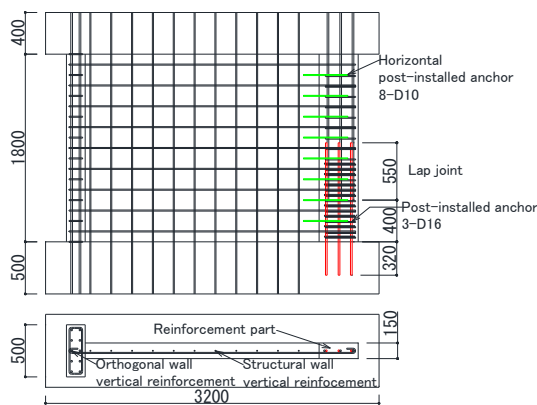
Table 6 The outline of the test pieces      Table 7 The results of testing the concrete materials

Test piece	TYPE-A1	TYPE-A2	TYPE-B
Orthogonal wall(mm×mm)	500×180		
Thickness of structural wall(mm)	150		
Length of structural wall(mm)	2620		
Height of wall (mm)	1800		
Orthogonal wall vertical reinforcement	D16(SD345)		
Orthogonal wall horizontal reinforcement	D10(SD295A)@200		
Structural wall vertical reinforcement	D10(SD295A)@200		
Structural wall horizontal reinforcement	D10(SD295A)@200		
Structural wall vertical reinforcement of reinforced part	3-D16(SD345)	2-D19(SD345) D10(SD295A)	
Structural wall horizontal reinforcement of reinforced part	D10(SD295A)@50		

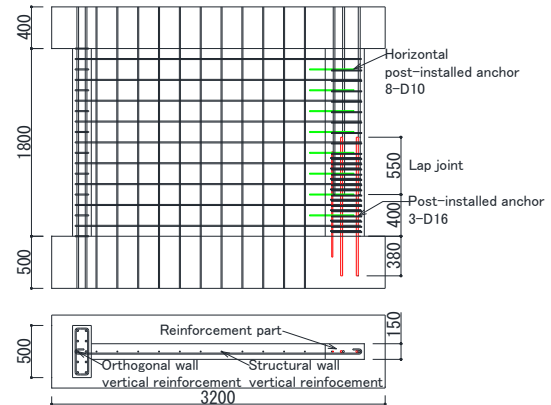
Test piece	Compressive strength (N/mm <sup>2</sup> )			Tensile strength (N/mm <sup>2</sup> )			Young's modulus (×10 <sup>3</sup> N/mm <sup>2</sup> )		
	Reinforced part	Existing part	Bottom stub	Reinforced part	Existing part	Bottom stub	Reinforced part	Existing part	Bottom stub
TYPE-A1	25.3	66.8	34.4	2.6	2.8	2.4	27.6	31.1	27.0
TYPE-A2		36.3			3.2			24.3	
TYPE-B									

Table 8 The results of testing the steel frame materials

Reinforcement	Young's modulus (×10 <sup>3</sup> N/mm <sup>2</sup> )	Yield strength (N/mm <sup>2</sup> )	Tensile strength (N/mm <sup>2</sup> )	Yield strain (×10 <sup>-6</sup> )
D10	181	356	487	1995
D16	184	372	543	2064
D19	179	373	554	2164



(a) TYPE-A1, A2



(b) TYPE-B

Fig. 9 The bar arrangement drawing of the test pieces

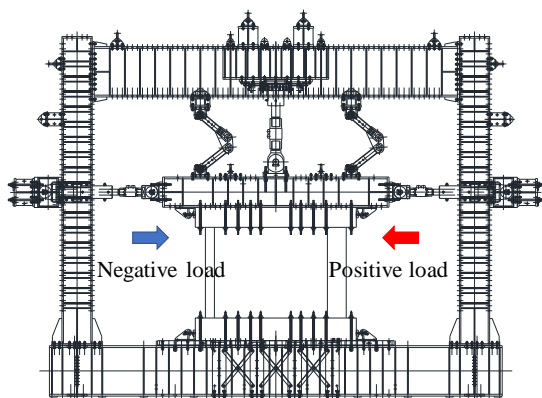
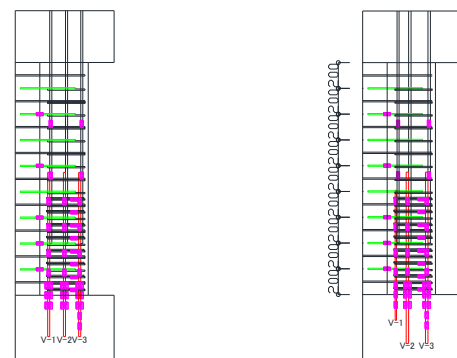


Fig. 10 The setup of the force-application device



(a) TYPE-A1, A2

(b) TYPE-B

Fig. 11 The position of the strain gauge



0.09%, followed by the post-installed anchor reinforcement at  $R = 0.12\%$  on the positive load side. On the side of the negative load, the hoop reinforcement first reached a tensile yield point at  $R = -0.42\%$ . Then, during the first cycle at  $R = -1.50\%$ , crushing occurred, with large shear cracks at the center of the structural wall, resulting in a sudden reduction in yield strength. The maximum yield strength was 720.8 kN at  $R = 0.76\%$  on the positive load side and -1187 kN at  $R = -0.75\%$  on the negative load side. On both positive and negative load sides, a failure mode was reached at the calculated values of the flexural strength. However, on the side of the negative load, an abrupt reduction in yield strength because of the widening of shear cracks was found. Therefore, the failure mode on the positive load side was a flexural failure, while that on the negative load side was a shear failure following flexural yielding.

In the case of TYPE-B, the vertical reinforcement in the structural wall first reached a tensile yield point at  $R = 0.15\%$ , followed by the post-installed anchor reinforcement at  $R = 0.30\%$  on the positive load side. On the side of the negative load, the hoop reinforcement first reached a tensile yield point at  $R = -0.04\%$  and the post-installed anchor reinforcement reached a tensile yield point at  $R = -0.08\%$ . Then, during the second cycle at  $R = 1.00\%$ , crushing occurred, with large shear cracks at the center of the structural wall, resulting in a sudden reduction in yield strength. The maximum yield strength was 1200.4 kN at  $R = 0.50\%$  on the positive load side and -697.9 kN at  $R = -0.44\%$  on the negative load side. On both positive and negative load sides, a failure mode was reached at the calculated values of the flexural strength. However, on the side of the positive load, an abrupt reduction in yield strength because of the widening of shear cracks was found. Therefore, the failure mode on the positive load side was a shear failure following flexural yielding, while that on the negative load side was a flexural failure.

For all test pieces of horizontal post-installed anchors, no yield with a higher of 600 mm or less was observed. In these test pieces, the horizontal post-installed anchors at the top exhibited greater strain than those at the bottom, possibly because of a larger load.

#### 4.4 Discussion

##### 4.4.1 Fixing performance of the post-installed anchors at the leg

Fig. 13 and Fig. 14 show the stress distributions and bonding stress distributions of TYPE-A under the positive load and TYPE-B under the negative load at peaks. In these figures, the result of the post-installed anchor removal test in Section 3 is indicated with dotted lines as bonding strength. The experimental values of bonding strength were obtained using Eq. (7).

$$\tau_1 = \frac{|T_1 - T_2|}{\pi \cdot D \cdot L_1} \quad (7)$$

Here,  $T_i$ : Tensile force ( $= E_S A \mu_i$ ) at  $T_i$ ;  $E_S$ : Young's modulus of each rebar;  $A$ : Cross-sectional area of each rebar;  $\mu_i$ : Strain of each rebar;  $D$ : Perimeter of each rebar;  $L$ : Fixing length

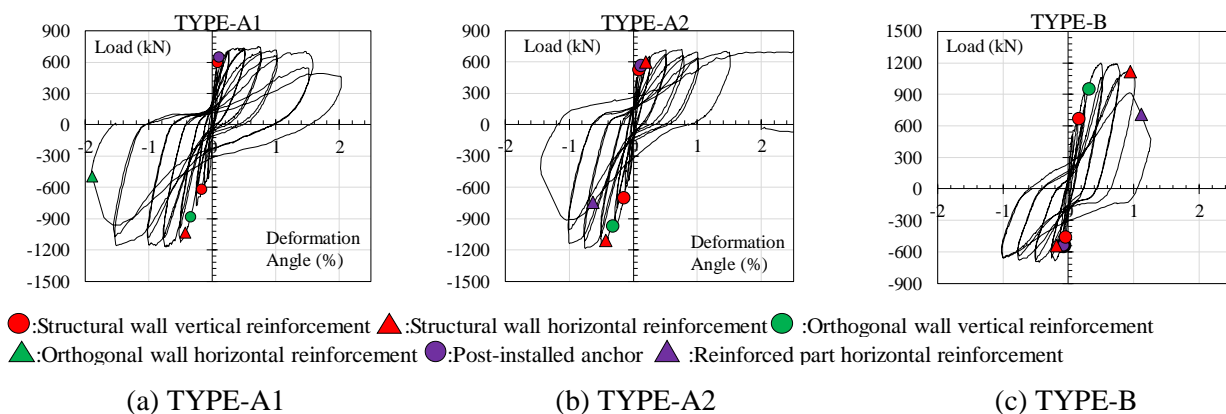


Fig. 12 The relationship between load and deformation angle



No test pieces reached the bonding strength, suggesting that a bonding failure did not occur. This demonstrates that for the long-span structural wall used for this experiment, by providing a burying length of 20 da, applying post-installation adhesive anchors to flexural reinforcement is effective.

#### 4.4.2 Evaluation of the backbone curves concerning load deformation

For the evaluation of a structural wall with the opening reinforced, the accuracy of the evaluation expressions presented in [2–5] was determined. Fig. 15 compares the calculated backbone curves and experimental values, and Table 9 lists the accuracy of the calculated values. The flexural ultimate strength of the backbone curves was obtained using Eq. (8) presented in [4], and the yield point rigidity reduction rate was obtained using Eq. (9), as indicated in [2, 4]. The shear ultimate strength was calculated using Eq. (10) presented in [5]. The bending crack strength and shear crack strength were calculated using Eq. (11) and (13), respectively, as indicated in [3].

$$M_u = A_{st}\sigma_{st}d - A_{sc}\sigma_{sc}d_c - \frac{\sigma_{av}b\beta_1x_n}{2} + Ng \quad (8)$$

Here,  $A_{st}$ : Cross-sectional area of each rebar on the pulling side of the neutral axis;  $\sigma_{st}$ : Intensity of stress of the rebars on the pulling side of the neutral axis;  $d$ : Distance from the compression edge to each rebar on the pulling side;  $A_{sc}$ : Cross-sectional area of each rebar on the compression side of the neutral axis;  $\sigma_{sc}$ : Intensity of stress of the rebars on the compression side of the neutral axis;  $d_c$ : Distance from the compression edge to each rebar on the compression side;  $g$ : Distance from the compression edge to the center of gravity axis;  $x_n$ : Distance from the compression edge to the neutral axis;  $\sigma_{av}$ : Average intensity of stress;  $N$ : Axial force

$$\alpha_y = \frac{{}_wM_y C_n}{E_c I_w \varepsilon_y} \quad (9)$$

Here,  ${}_wM_y$ : Flexural moment at the yield of the vertical reinforcement on the 3rd column from the reinforced part or the 2nd column from the end of the side of the orthodox wall.  $C_n$ : Distance from the elastic neutral axis to the vertical reinforcement on the 3rd column from the reinforced part or the 2nd column from the end of the side of the orthodox wall at the yield of that vertical reinforcement;  $E_c$ : Young's modulus of the concrete;  $I_w$ : Cross-sectional second moment;  $\varepsilon_y$ : Yield strain of the main reinforcement members at the end of the reinforcement or at the end on the orthodox wall.

$$Q_{su} = \left\{ \frac{0.068 p_{te}^{0.23} (F_c + 18)}{\sqrt{M/(QD) + 0.12}} + 0.85 \sqrt{p_{wh} \sigma_{wh}} + 0.1 \sigma_0 \right\} t_e j \quad (10)$$

Here,  $p_{te}$ : Ratio of the tension reinforcement in the equivalent cross-section;  $F_c$ : Strength of the concrete;  $\sigma_{wh}$ : Yield strength of the horizontal reinforcement;  $p_{wh}$ : Ratio of the horizontal reinforcement,

$\sigma_{wh}$ : Intensity of stress in the axial direction;  $t_e$ : Wall thickness;  $j$ : Distance between the center of tension and the center of the compression

$${}_sQ_{cr} = \frac{{}_s\tau_{cr} t_w l_w}{\kappa_s} \quad (11)$$

Here,  ${}_s\tau_{cr}$ : Shear intensity of stress at the occurrence of shear cracks;  $\sigma_t$ : Tensile strength of the concrete;  $\kappa_s$ : Shear form factor

$$M_c = (0.56 \sqrt{\sigma_B} + \sigma_0) Z_e \quad (13)$$

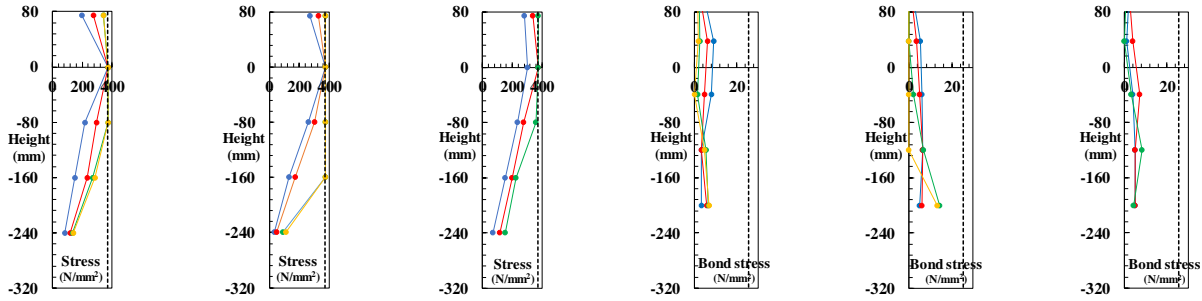
Here,  $\sigma_0$ : Intensity of stress in the axial direction;  $\sigma_B$ : Compressive strength of the concrete;  $Z_e$ : Equivalent cross-sectional coefficient of the wall plate while considering the reinforcement

$$\beta = \frac{0.46 p_w \sigma_y}{F_c} + 0.14 \quad (14)$$

Here,  $p_w$ : Vertical wall reinforcement ratio;  $\sigma_y$ : Yield strength of the vertical wall reinforcement;  $F_c$ : Compressive strength of the concrete



The rigidity reduction rates are almost the same, demonstrating that the maximum yield strength in the experimental values can be evaluated on the safe side.

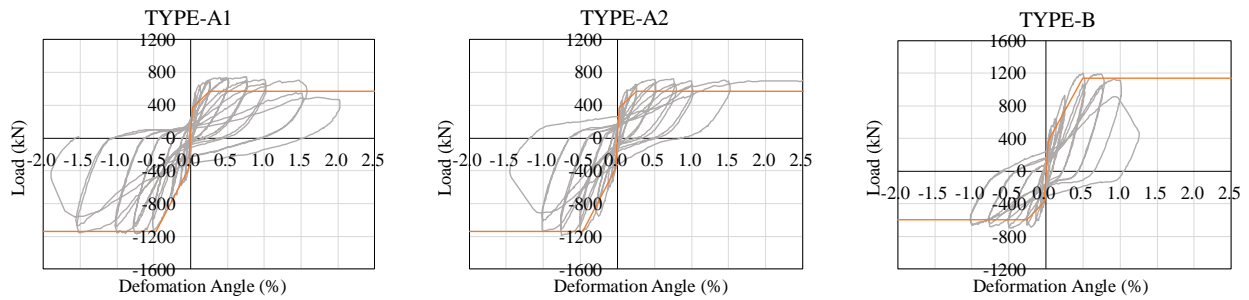


Explanatory notes : ●:0.13% ●:0.25% ●:0.50% ●:0.75%      Explanatory notes : ●:0.13% ●:0.25% ●:0.50% ●:0.75%

(a) TYPE-A1      (b) TYPE-A2      (c) TYPE-B      (a) TYPE-A1      (b) TYPE-A2      (c) TYPE-B

Fig. 13 The stress distributions

Fig. 14 The bonding stress distributions

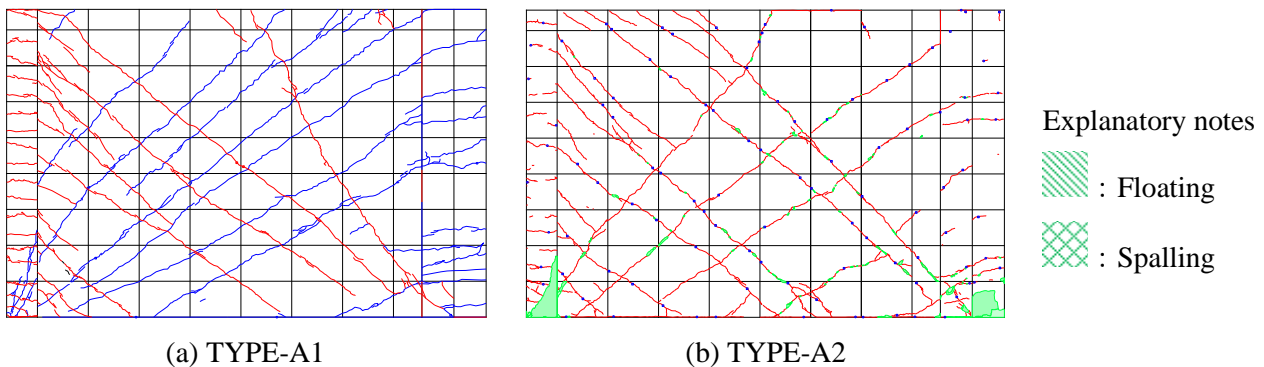


(a) TYPE-A1      (b) TYPE-A2      (c) TYPE-B

Fig. 15 The calculated backbone curves

Table 9 The accuracy of the calculated values

Test piece	Loading direction	Failure mode	Maximum load (kN)	Calculated values		Accuracy (Experimental value / Calculated value)
				Flexural ultimate strength (kN)	Shear ultimate strength (kN)	
TYPE-A-1	Positive load	Flexural failure	750	574	1124	1.31
	Negative load	Shear failure following flexural yielding	-1175	-1137	-1286	1.03
TYPE-A-2	Positive load	Flexural failure	721	574	1124	1.26
	Negative load	Shear failure following flexural yielding	-1187	-1137	-1286	1.04
TYPE-B	Positive load	Shear failure following flexural yielding	1200	1142	1293	1.05
	Negative load	Flexural failure	-689	-595	-1133	1.16



(a) TYPE-A1      (b) TYPE-A2

Fig. 16 A crack damage figure at deformation angle R = -1%



#### 4.4.3 Toughness of TYPE-A1 and TYPE-A2 under the Negative Load

Fig. 16 presents a crack damage figure at deformation angle  $R = -1\%$  during the cycle immediately before the cycle with a sudden reduction in yield strength of TYPE-A2. TYPE-A1 is superior to TYPE-A2 in toughness under the negative load. The failure mode of TYPE-A1 and TYPE-A2 under the negative load was a shear failure following the flexural yield. In both test pieces, the concrete in the reinforcing part crushed, and the widening of shear cracks at the center of the structural wall caused a sudden reduction in yield strength, tending to result in a shear failure. Because the concrete at the reinforcement of TYPE-A1 has high strength, crushing, one of the factors causing a shear failure, occurs at a deformation angle greater than that of TYPE-A2, possibly indicating improved toughness. At a deformation angle of  $-1\%$ , TYPE-A2 significantly exhibited floating and foiling at the leg of the reinforcement, indicating a sign of crushing. In contrast, TYPE-A1 had no floating or spalling at the leg of the reinforcement, as shown in Fig. 16.

### 5. Conclusion

In this research, experiments were conducted on wall girders and structural walls reinforced for a new opening, and the effects of reinforcement were evaluated, as well as the method for evaluating their structural performance. The following knowledge was gained through this research.

- It is generally possible to obtain the backbone curve of the relationship between load and deformation of the wall girders reinforced for installing an opening by a calculation using conventional evaluation equations.
- It was confirmed that B-3', with concrete placed on both sides and the bottom surface of the girders had smaller shearing between the conventional and reinforced parts and higher toughness.
- It is estimated that the difference in yield strength under the negative load between B-2' and B-3' in the wall girder experiment was caused by the large difference between the moments that act on the critical section position because the critical section position of B-3' was inside the stab.
- It is generally possible to obtain the backbone curve of the relationship between load and deformation of the structural wall reinforced for installing an opening by a calculation using conventional evaluation equations.
- It was confirmed that toughness was enhanced by using concrete with higher compressive strength at the reinforcement.

### 5. Acknowledgement

This research was conducted as a part of "Development of the Technology for Enlarging the Spaces in Existing Medium- and Low-Rise Reinforced Concrete Buildings," a research theme of Building Research Institute (BRI). The experiments were performed at an experimental facility of the BRI Strength Test Building. We express our gratitude to the parties concerned.

### 7. References

- [1] Y. Hibino (2008): Structural Retrofit for Reduced RC Beams in Existing Buildings, Summaries of Technical Papers of Annual Meeting, Architectural Institute of Japan, Structures-IV, pp.97-100
- [2] Y. Maruyama (2018): Structural Performance Evaluation for Existing Box Wall Structure with Structural Renovation Part1; Investigation by experimental test for structural wall, Summaries of Technical Papers of Annual Meeting, Architectural Institute of Japan, Structures-IV, pp.417-418
- [3] Architectural Institute of Japan (2015): All Standard for Design and Calculation of Reinforced Concrete Box-shaped wall Structures
- [4] Architectural Institute of Japan (1997): Design Guidelines for Earthquake Resistant Reinforced Concrete Buildings Based on Inelastic Displacement Concept (Draft)
- [5] National Institute for Land and Infrastructure Management (NILIM) and Building Research Institute (BRI) (2015): Commentary on Structural Regulations in the Building Standard Law of Japan.